

Antiferromagnetism, valence fluctuation, and heavy-fermion behavior in $\text{EuCu}_2(\text{Ge}_{1-x}\text{Si}_x)_2$ Z. Hossain,¹ C. Geibel,¹ N. Senthilkumaran,¹ M. Deppe,¹ M. Baenitz,¹ F. Schiller,² and S. L. Molodtsov²¹Max Planck Institut für Chemische Physik fester Stoffe, Nöthnitzer Strasse 40, 01187 Dresden, Germany²Institut für Festkörperphysik, Technische Universität Dresden, 01062 Dresden, Germany

(Received 31 March 2003; revised manuscript received 17 October 2003; published 30 January 2004)

We have investigated the magnetic, thermodynamic, transport, and electronic properties across the transition from the divalent antiferromagnetic state to the valence fluctuating state of Eu in the alloy $\text{EuCu}_2(\text{Ge}_{1-x}\text{Si}_x)_2$. The antiferromagnetic state is very stable from $x=0$ up to $x=0.6$ and disappears rather abruptly at $x_c \approx 0.65$. Near the crossover, we confirmed a pronounced Kondo-like behavior in the resistivity and in the thermopower. Further on, for x slightly larger than x_c , we observe the formation of a heavy Fermi liquid at low temperatures, as evidenced by a large linear coefficient of the specific heat ($\gamma=191$ mJ/K² mol for $x=0.7$), a large quadratic term in the resistivity and a strongly enhanced constant susceptibility χ_0 . This is a unique observation of heavy fermion behavior in a Eu compound. The photoemission spectra of the Eu $4f$ and $3d$ core levels indicate significant valence fluctuation even for $x < x_c$ in the magnetically ordered regime. The decrease of T_N before reaching the critical point as well as the Kondo and the heavy fermion behavior found near x_c are in strong contrast to the observation in typical Eu systems, which usually show a first-order transition from a (almost) divalent state to a strongly valence fluctuating Eu state.

DOI: 10.1103/PhysRevB.69.014422

PACS number(s): 75.30.Mb, 75.30.Kz, 75.50.Ee

I. INTRODUCTION

The transition from a magnetically ordered ground state to a nonmagnetic ground state is presently one of the hot research topics in the field of condensed matter physics. This is due to the fact that in several systems the disappearance of the magnetic order results in very interesting phenomena, like, e.g., formation of heavy fermions, onset of unconventional superconductivity, and appearance of non-Fermi-liquid behavior.¹ Within intermetallic compounds, such investigations have been carried out mostly on Ce- or U-based systems. Since these elements present an unstable f shell, they can quite easily be tuned from a magnetic to a nonmagnetic state by alloying or applying pressure. Increasing the hybridization g between the localized f and the conduction electrons leads to a weakening of the magnetic order, which eventually disappears at a critical strength g_c . In Ce- and U-based systems, increasing g always leads, within some range of g below g_c , to a continuous and significant (at least by a factor of two) decrease of the magnetic ordering temperature T_m . In many systems, it is even suggested that T_m continuously decreases down to $T=0$ K, leading to a quantum critical point.²⁻⁵

Eu also presents an unstable f shell, since it can switch between the divalent, magnetic ($J=7/2$), and the trivalent, nonmagnetic ($J=0$) configuration. However, the magnetic phase diagram observed upon tuning g is very different from that found in Ce- and U-based systems. Starting from a stable divalent Eu systems, one never observes a decrease of T_m with increasing g . Instead T_m seems to be independent of g or even to increase slightly with g , until the system makes at g_c a pronounced first-order transition to a valence fluctuating state, with a valence close to three.^{6,7} Since at $g \geq g_c$ the characteristic energy associated with the valence fluctuation is quite high, the mass enhancement of the conduction electron is comparatively small in Eu systems. Thus, no Eu-based heavy fermion system has yet been found. Further on,

whereas Kondo behavior in transport properties, i.e., a pronounced increase of the magnetic scattering with decreasing temperature, is ubiquitous in Ce- and U-based systems, no such behavior has yet been observed in Eu-based systems, with only one exception, namely $\text{EuCu}_2(\text{Ge}_{1-x}\text{Si}_x)_2$.⁸ In this system, exchanging Ge by Si induces a transition from a divalent, antiferromagnetic ordered state in pure EuCu_2Ge_2 ⁹ to a valence fluctuating state in pure EuCu_2Si_2 .¹⁰ In the first investigation of this system, Levin *et al.*⁸ observed Kondo-like behavior in the temperature dependence of the resistivity and of the thermopower for $0.4 < x < 0.8$. Further investigations did not add much information.^{11,12} Noteworthy, the thermodynamic properties have never been reported, and the evolution of the magnetic order in the system has also not been investigated. In order to have a more precise view of this unusual Eu system, we present in this paper a detailed investigation of its magnetic susceptibility, resistivity, thermopower, and specific heat. In addition, valence fluctuation was studied with core-level and valence-band photoemission (PE) spectroscopy. Our results allow us to draw a precise magnetic phase diagram and demonstrate the formation of a heavy Fermi-liquid state for x slightly larger than x_c (critical concentration where magnetic order disappears), a unique observation of a Eu-based heavy fermion system.

II. EXPERIMENT

Polycrystalline samples of $\text{EuCu}_2(\text{Ge}_{1-x}\text{Si}_x)_2$ were prepared by arc melting the constituent elements followed by annealing for 1 week at 800–900°C. Powder x-ray diffraction patterns confirm that the samples form in the ThCr_2Si_2 -type tetragonal structure (space group $I4/mmm$). Our lattice parameters agree very well with those of Ref. 8. While a decreases almost linearly over the whole concentration range (by 3.7% from $x=0$ to $x=1$), the decrease of c is slowed down for $x > 0.6$. Thus, the volume also decreases continuously from $x=0$ to $x=1$, while the ratio a/c is es-

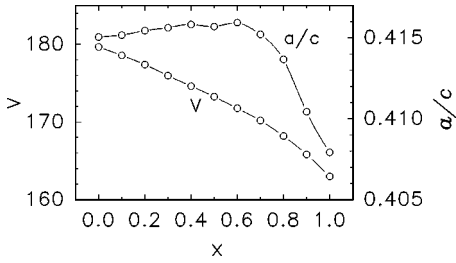


FIG. 1. Composition dependence of the unit-cell volume $V(\text{\AA}^3)$ and of (a/c) of $\text{EuCu}_2(\text{Ge}_{1-x}\text{Si}_x)_2$.

essentially constant up to $x=0.6$, above which it decreases (Fig. 1). The quality of our samples seems to be better than those in the previous investigations,^{8,12} since our samples present larger ordering temperatures, much better defined anomalies at the antiferromagnetic transition and a more pronounced temperature dependence in the resistivity. We studied the compositional homogeneity for the sample with $x=0.6$, using electron probe microanalysis (EPMA). The deviation of the Si/Ge ratio from the expected value was less than 1% for different parts of the sample. Magnetization measurements were carried out using a commercial superconducting quantum interference device (SQUID) magnetometer. Electrical resistivity (ρ), thermoelectric power (S), and specific heat (C) measurements were carried out using a commercial physical property measurement system (PPMS, Quantum Design).

Photoemission experiments were performed with a SCI-ENTA 200 electron-energy analyzer using monochromatized light from a He discharge lamp ($h\nu=21.2$ eV [He I α] and 40.8 eV [He II α]) and a x-ray source with a Al anode ($h\nu=1486.7$ eV [Al K α]). The total energy resolution was set to 25 meV full width at half maximum (FWHM) and to 400 meV FWHM in the ultraviolet (UPS, He I α and He II α) and the x-ray (XPS, Al K α) photoelectron spectroscopy modes, respectively. The surfaces of the samples were cleaned with a diamond file until no traces of oxygen or carbon contaminations were observed both in valence-band and core-level PE spectra. The samples were mounted onto a He/N₂ cryostat allowing for cooling to temperatures of 4 K and 77 K with liquid He and N₂, respectively. PE spectra were taken at the two above temperatures and room temperature in ultrahigh vacuum conditions with a pressure in the range of 1×10^{-10} mbar. The pressure rose shortly to 5×10^{-10} mbar upon filing of the sample surfaces.

III. RESULTS AND DISCUSSION

A. EuCu_2Ge_2

We first focus on pure EuCu_2Ge_2 , since a comprehensive report on its properties has not yet been published. Above 20 K, its susceptibility follows a Curie-Weiss law with $\theta_p = -30$ K and an effective moment $7.8 \mu_B$, which is very close to the value expected for divalent Eu^{2+} ions. A pronounced change of the slope indicates the transition into an antiferromagnetic state at Néel temperature $T_N=14$ K (Fig. 2). $\chi(T)$ decreases only very slightly below T_N and is essentially tem-

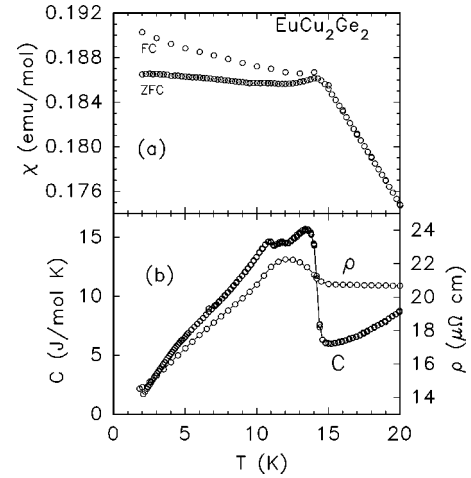


FIG. 2. (a) Magnetic susceptibility (χ) measured at 0.1 T under zero-field-cooled (ZFC) and field-cooled (FC) conditions. (b) Resistivity (ρ) and specific heat (C) of EuCu_2Ge_2 at low temperatures. Distinct anomalies due to magnetic transitions are seen.

perature independent below 12 K. The rather small decrease of $\chi(T)$ below T_N is in accordance with the weak anisotropy expected for the pure spin state of the $4f^7$ configuration. There is a small difference between the zero-field-cooled (ZFC) and the field-cooled (FC) susceptibility below 14 K, whose origin is not yet clear. In contrast, the magnetization is almost linear up to 5.5 T, both in the paramagnetic ($T=25$ K) and in the antiferromagnetic ($T=2$ K) state. From room temperature down to 15 K, $\rho(T)$ follows the behavior of a classical metal, i.e., a linear dependence at higher temperature merging in a constant resistivity at low temperature. At T_N , $\rho(T)$ shows a distinct increase, reaching a maximum at 12 K, and decreasing again considerably down to 2 K (Fig. 2). The spin density wave (SDW) like increase in $\rho(T)$ at T_N indicates the formation of an energy gap at the Fermi surface, likely to be a superzone gap due to the antiferromagnetic ordering.¹³ The specific-heat data reveal a sharp mean-field-type anomaly at $T_N=14$ K and two further small anomalies at 11.5 K and 11 K, respectively. We suspect that these two small anomalies are related to change of the spin arrangements within the antiferromagnetic state. A second transition in this temperature range was also reported by Fukuda *et al.*¹² Below these anomalies, $C(T)$ decreases linearly with the temperature with a large coefficient, as observed in many Gd and divalent Eu-based systems. This behavior is related to the large degeneracy of the $S=7/2$ state.¹⁴ The above results confirm the antiferromagnetic order at $T_N=14$ K and the stable divalent Eu state in EuCu_2Ge_2 .

B. $\text{EuCu}_2(\text{Ge}_{1-x}\text{Si}_x)_2$

The previous investigations of this alloy indicate that the Eu valence remains close to 2^+ for $x \leq 0.6$, but increases rather strongly with the Si content for $x \geq 0.7$. This is, e.g., evidenced in the evolution of the susceptibility $\chi(T)$. Our results, which also agree with previous investigations,^{8,12} are shown for selected samples in Fig. 3. For $x \leq 0.6$, $\chi(T)$ follows a Curie-Weiss law from 300 K down to 30 K, with an

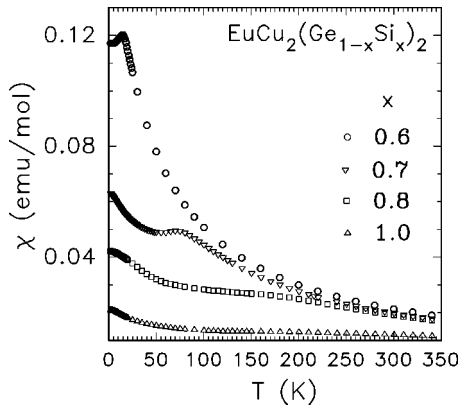


FIG. 3. Magnetic susceptibility of $\text{EuCu}_2(\text{Ge}_{1-x}\text{Si}_x)_2$ for selected samples. Peak in χ for $x=0.6$ sample is due to magnetic order. No anomaly due to magnetic order is observed for $x=0.7$. The χ for $x=0.7, 0.8$, and 1.0 show broad maxima due to valence fluctuation.

effective moment close to the value for a free Eu^{2+} ion and low θ_p values (< -40 K). A clear kink between 15 and 20 K is observed indicating the onset of magnetic order in this concentration range. In contrast, for samples with $x \geq 0.7$, $\chi(T)$ deviates strongly from a Curie-Weiss law below 100–200 K, showing a broad maximum and much smaller absolute values, as expected for intermediate valent systems. The θ_p values estimated from Curie-Weiss fit increase only slightly with x for $x < 0.7$, from $\theta_p = -30$ K in pure EuCu_2Ge_2 to $\theta_p = -44$ K at $x=0.6$. For $x > 0.7$, the slope $d\theta_p/dx$ becomes much larger in accordance with the strong increase of valence fluctuations. However, since a reliable determination of θ_p would require measurements up to much higher temperatures, above 400 K, we cannot give absolute numbers here. Levin *et al.*⁸ suggested that the valence v increases in two steps, the first step at $x=0.5$, from $v=2$ to $v=2.15$, and the second step at $x=0.9$, from $v=2.15$ to $v=2.4$, v being almost constant for $0.6 < x < 0.9$. Our results indicate that this two-step increase of v and the constant value of v in the intermediate concentration range is likely due to a misinterpretation of the peak in $\rho(T)$ and $S(T)$. The authors did not investigate the evolution of the antiferromagnetic order and were thus not aware of the magnetic ordered state in the intermediate concentration range. Our results suggest a rather continuous increase of the valence fluctuation over the whole concentration range (at least for $x > 0.4$), the slope itself increasing with the Si content.

1. Evolution of the antiferromagnetic order

The most precise information on the evolution of the antiferromagnetic state stems from the specific-heat measurements. For $0 < x < 0.6$, the transition at T_N remains very sharp, the size of the anomaly at T_N stays constant, but T_N shifts continuously to higher temperatures, reaching a maximum at $x=0.5$ with $T_N=20$ K [Fig. 4(a)] (see also phase diagram in Fig. 9). Thus, despite the disorder introduced by alloying, the long-range antiferromagnetic order is very well preserved and becomes even more stable with increasing Si

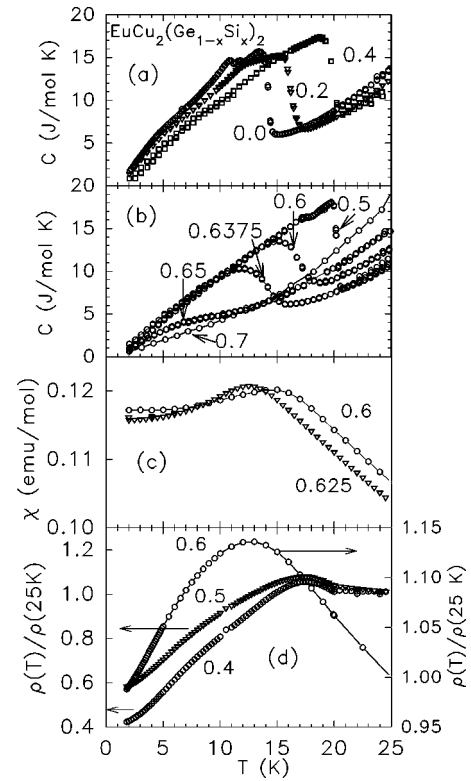


FIG. 4. (a) Specific heat of $\text{EuCu}_2(\text{Ge}_{1-x}\text{Si}_x)_2$ for $x \leq 0.4$ showing anomalies due to magnetic order. (b) Specific heat for $0.5 \leq x \leq 0.7$. Well-defined anomalies due to magnetic order is found for $x \leq 0.6325$, the anomaly is drastically reduced for $x=0.65$ and disappears for $x=0.7$. (c) Anomalies in the magnetic susceptibility is observed even in samples which are quite close to the critical concentration. (d) Resistive anomalies due to magnetic transition for $x=0.4, 0.5$, and 0.6 . The resistivity increase at $T_N \approx 20$ K for $x=0.4$ and 0.5 is due to superzone gap formation.

content. The weaker anomalies observed near 12 K at $x=0$ get more pronounced at $x=0.2$, but disappear at higher concentration, suggesting a complex magnetic phase diagram within the antiferromagnetic state. For $x > 0.5$ a pronounced evolution of the magnetic order sets in [Fig. 4(b)]. T_N decreases faster and faster, down to $T_N=14$ K at $x=0.6375$, and the size of the anomaly in $C(T)$ at T_N also decreases (to 50% of its value at lower x). The width of the anomaly increases slightly, but even at $x=0.6375$, the anomaly is still well defined, clearly indicating a long-range order. The slight broadening of the anomaly can easily be accounted for by the combination of the large slope dT_N/dx and an inhomogeneity of the Si distribution of the order of 1%, which is difficult to avoid in such an alloy system. At $x=0.65$ no clear anomaly is observed. One could suspect that the very weak and very broad bump in the $C(T)$ curves near 8 K corresponds to a strongly broadened transition, but this would require a sudden and large increase of dT_N/dx . Transforming this broad anomaly to a sharp one would also lead to a further strong reduction of the size of the anomaly compared to that at $x=0.6375$.

No anomaly, even a broad one, can be resolved for $x > 0.65$. Thus, the antiferromagnetic order is suppressed at a

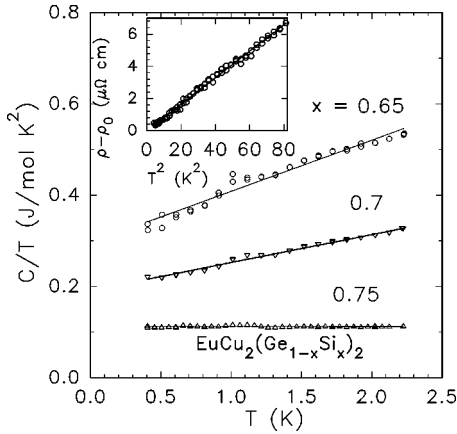


FIG. 5. C/T vs T for samples with $x \geq x_c$ demonstrating the large linear electronic contribution to the specific heat. Inset shows T^2 dependence of $(\rho - \rho_0)$ for $x=0.7$ in the temperature range 2–9 K.

critical point near $x_c=0.65$, although we cannot tell unambiguously whether it is a quantum critical point ($T_N \rightarrow 0$ K) or a classical critical point at a finite temperature [$T_N(x \rightarrow x_c) \approx 13$ K]. The sharpness of the transition, close to the critical concentration, shows that the long range nature of the magnetic order is preserved until the critical point. If there is a concentration region where some part of the sample orders magnetically while other parts do not, the width of this region is very narrow, at most 2 at. % of Ge. Our results further indicate a significant decrease of T_N before reaching the critical point, in contrast to the observation in other Eu-based system where T_N stays constant or even increases until the critical point.

The evolution of the anomalies in $\rho(T)$ and $\chi(T)$ with x [Figs. 4(c) and 4(d)] confirms the concentration dependence of T_N found in the $C(T)$ measurements. The SDW-like increase of $\rho(T)$ at T_N is well defined until $x=0.5$ [Fig. 4(d)]. For $x=0.6$, the Kondo-like increase of $\rho(T)$ (see below) becomes so strong that the SDW-like increase at T_N cannot be discerned anymore. However, the maximum in $\rho(T)$ slightly below T_N is still well defined. The anomaly in $\chi(T)$ is also very well defined at $x=0.6$ and $x=0.625$. The anomalies we observed at T_N in this concentration range are much more pronounced than those reported by Fukuda *et al.*,¹² indicating a better homogeneity and thus higher quality of our samples as evidenced by EPMA.

2. Heavy fermion behavior

The specific-heat data for the $x=0.7$ sample in Fig. 4(b) already suggest that below 10 K $C(T)$ is dominated by a linear contribution. Therefore, for the samples at or slightly above the critical concentration $C(T)$ was measured down to 0.4 K and the results were plotted as C/T versus T in Fig. 5. In this plot the data for $x=0.65$, 0.7, and 0.75 follow a straight line between 0.4 K and 2 K. Thus, the temperature dependence of the specific heat can be described by $C = \gamma T + \delta T^2$, the linear term, which is the dominant one, decreases with increasing Si content from $\gamma=296$ mJ/K² mol for $x=0.65$ to $\gamma=191$ mJ/K² mol for x

$=0.7$ and $\gamma=113$ mJ/K² mol for $x=0.75$. These results suggest the formation of heavy quasiparticles at low temperatures in these samples. This is confirmed by an analysis of the resistivity and susceptibility of the $x=0.7$ sample. At low temperatures ($T < 10$ K), the resistivity shows T^2 dependence, as expected for a Fermi liquid (inset in Fig. 5). A fit $\rho(T) = \rho_0 + AT^2$ leads to $A = 0.082$ $\mu\Omega$ cm/K². Many Ce- and U-based heavy fermion systems follow a universal relation $A \propto \gamma^2$ which is known as Kadowaki-Woods relation,¹⁵ with a mean value for the ratio A/γ^2 of the order of 1×10^{-5} [$\mu\Omega$ cm(mol K/mJ)²]. For $\text{EuCu}_2(\text{Si}_{0.7}\text{Ge}_{0.3})_2$, we get $A/\gamma^2 = 2.25 \times 10^{-6}$ [$\mu\Omega$ cm(mol K/mJ)²], which is a factor of four lower than this mean value. An even lower value of 0.4×10^{-6} [$\mu\Omega$ cm(mol K/mJ)²] has been reported in some Yb-based intermediate valent systems, and suggested to be related to the larger ground-state degeneracy of these systems,¹⁶ which is also the case for Eu^{2+} ($N=8$). This explanation has been recently supported by a theoretical work, which for a heavy fermion system with N -fold degeneracy predicts a reduction of the Kadowaki-Woods ratio by a factor which can be as large as $N(N-1)/2$, depending on the coupling strength.¹⁷ Thus, the A/γ^2 ratio we observed in $\text{EuCu}_2(\text{Si}_{0.7}\text{Ge}_{0.3})_2$ is in between the value observed and expected for heavy fermion systems with a doublet ground state, and that observed and expected for intermediate valent systems with a large ground-state degeneracy. A further test for the heavy fermion behavior is given by the Wilson ratio $W = \chi_0 \pi^2 k_B^2 / (\gamma \mu_{eff}^2)$ between the value of the constant susceptibility χ_0 at low temperatures and γ . In heavy fermion systems, the magnetic and the thermal excitations are comparably enhanced and W is found to be close to unity. With χ and γ determined at 1.8 K, the Wilson ratio for $\text{EuCu}_2\text{Ge}_{0.6}\text{Si}_{1.4}$ ($x=0.7$) is 1.15. Therefore, we observed in this compound at low temperatures an enhanced linear term in the specific heat, which correlates with an enhanced coefficient of the quadratic term in the resistivity and with an enhanced constant susceptibility, proving the formation of a heavy Fermi-liquid state in this system. These results clearly demonstrate that it is possible to find heavy fermion behavior in Eu compounds as well.

In Ce- and Yb-based heavy fermion systems, when approaching the critical point where the magnetic order is suppressed, one generally observes at low temperatures an additional contribution in $C(T)$ besides the enhanced linear term. However, this contribution always increases with decreasing temperature, in contrast to our results for $x=0.65$ and $x=0.7$ samples. They show an additional positive term proportional to δT^2 , which is thus decreasing with decreasing temperature. Since this quadratic term decreases when going away from the critical point, from $\delta=112$ mJ/K³ mol for $x=0.65$ to $\delta=62$ mJ/K³ mol for $x=0.7$, and disappears for $x=0.75$, it should be related to the critical point. However, we are not aware of an appropriate theory for this behavior.

Since for $x=0.7$, Eu valency is close to 2^+ , a rough estimate of the Kondo temperature can be obtained from the specific-heat and magnetic-susceptibility data using Coqblin-Schrieffer model. According to this model, the Kondo tem-

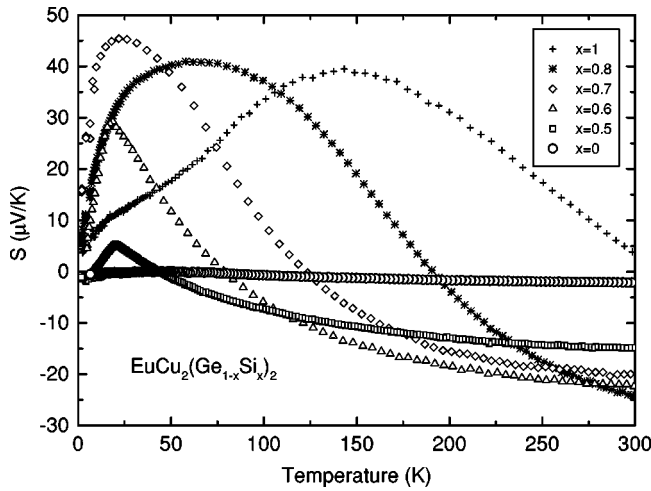


FIG. 6. Temperature dependence of thermopower for selected samples.

perature $T_K = (N-1)\pi R/(6\gamma)$, where $N=2J+1$, $R=8.314 \text{ J}/(\text{mol K})$, and γ is the linear coefficient of specific heat.¹⁸ Using $\gamma=191 \text{ mJ}/\text{mol K}^2$ we obtain $T_K=160 \text{ K}$. Further, in this model, the magnetic susceptibility for $J=7/2$ exhibits a maximum at roughly $T_K/4$. For $x=0.7$, we observed in the magnetic susceptibility a broad maximum around 75 K corresponding to $T_K \approx 300 \text{ K}$. Thus, both T_K 's are of the same order of magnitude, but the value estimated from the susceptibility is a factor of two larger than that estimated from the specific heat, which is itself larger than the temperatures of the maxima observed in the resistivity or thermopower (see below). These differences suggest that this model is only a crude approach to this Eu-heavy fermion system, and that more sophisticated models are needed for a precise description. For higher Si concentration ($x>0.7$) the Kondo temperature rapidly increases as evidenced by large reduction of the γ value and large shift of the thermopower maximum to higher temperatures (see Fig. 6).

3. Kondo behavior

The observation of Kondo behavior in $\rho(T)$ and $S(T)$ was already reported by Levin *et al.*⁸ Nevertheless, we shall present and discuss our results, since our data are more extended and more precise and our conclusions are partially different. In samples with $x<0.5$, $\rho(T)$ follows the behavior typical for compounds with stable f electrons, i.e., an almost linear decrease of $\rho(T)$ with T at high temperatures due to phonon scattering, merging in a temperature independent $\rho(T)$ below 50 K due to spin and defect scattering, and a pronounced decrease at T_N due to the suppression of the spin disorder scattering [Fig. 7(a)]. Kondo-like behavior, i.e., an increase of $\rho(T)$ with decreasing temperatures, first appears in the sample $x=0.5$ and becomes already very pronounced in the sample with $x=0.6$, where $\rho(T)$ increases by 50% between a minimum in $\rho(T)$ around 100 K and a peak around 13 K. Comparison with $\rho(T)$ at lower concentrations and with the specific-heat data indicate that this maximum is related to the onset of the antiferromagnetic order, and do not correspond to the Kondo maximum as suggested by Levin

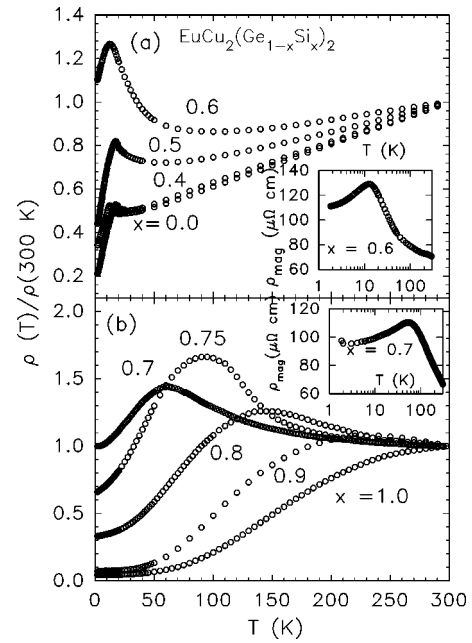


FIG. 7. (a) Temperature dependence of the resistivity (ρ) for $x < x_c$ where magnetic order is observed. Inset shows $\ln T$ dependence of the magnetic part of the resistivity for $x=0.6$. (b) Temperature dependence of the resistivity for $x > x_c$ where magnetic order has disappeared. Inset shows $\ln T$ dependence of the magnetic part of the resistivity for $x=0.7$.

*et al.*⁸ Therefore, for $x<0.7$, the temperature of this maximum is not T_K . At $x=0.7$, this rather sharp maximum has transformed into a broader maximum at a much higher temperature, and it shifts further to higher temperature with increasing Si content [Fig. 7(b)]. The increase of $\rho(T)$ for $x=0.6$ and 0.7 is proportional to $\ln T$ in a rather broad temperature range (insets of Fig. 7), as expected for Kondo scattering. The Kondo-like increase is still rather pronounced for $x=0.75$, but becomes weaker and weaker with further increasing Si content, $\rho(T)$ showing now the behavior typical for a valence fluctuating system. In this concentration range ($x \geq 0.7$), the position of the maximum is likely related to the characteristic energy scale of the valence fluctuations T_f .

The behavior of the thermopower $S(T)$ corresponds nicely to the behavior observed in the resistivity. In pure EuCu_2Ge_2 , the absolute value of $S(T)$ is very small ($|S(T)| < 2 \mu\text{V}/\text{K}$) in the whole temperature range. $S(T)$ is negative at high temperatures and exhibits a kink at T_N . For $x=0.5$ the absolute value has increased significantly and $S(T)$ shows a characteristic temperature dependence, which is preserved until pure EuCu_2Si_2 . Starting from a large negative value at 300 K, $S(T)$ changes sign at $T_s=40 \text{ K}$, and presents a very sharp peak at T_N . With increasing x , the negative value at 300 K also increases, the temperature T_s at which $S(T)$ changes sign shifts to higher temperatures and the increase of $S(T)$ for $T < T_s$ becomes more and more pronounced. For $x=0.6$, this increase also ends into a sharp peak at T_N , whereas for $x=0.7$ it merges into a broad maximum at $T_{Smax}=22 \text{ K}$, which shifts to higher temperature with further increasing x . Thus, as in resistivity, for $x<0.7$ the temperature of the peak in $S(T)$ does not correspond to

TABLE I. The temperature of resistivity maximum [$T_{\rho max}$ (K)], thermopower maximum [T_{Smax} (K)], and thermopower change of sign [T_s (K)] for different x .

x	$T_{\rho max}$ (K)	T_{Smax} (K)	T_s (K)
1.0	>300	145	>300
0.8	140	65	185
0.7	60	22	125
0.6	<15	<20	80

the Kondo temperature, as suggested by Levin *et al.*,⁸ but to T_N . On the other hand, for $x \geq 0.7$, the temperature of the broad maximum is also likely related to the characteristic energy of the valence fluctuations. It seems that the temperature dependence of the thermopower, i.e., the crossover from a large negative value at high temperature ($T > T_K$) to a large positive maximum at lower temperatures ($T < T_N$) is in accordance with prediction of the Kondo model for Eu ions.¹⁹ The magnetoresistance for samples with $0.5 \leq x \leq 0.7$ shows similar behavior as in the Ce-based Kondo lattice system.¹¹

The characteristic valence fluctuation energy scale (or the Kondo energy) is reflected in three different temperatures, $T_{\rho max}$, T_{Smax} , and T_s (Table I). However, although all of them shift to higher temperatures with increasing x , the slope is different. Thus, in the absence of a reliable theory, we cannot determine absolute values for T_K . However, the shift of T_s to even lower values when x decreases from $x=0.7$ to $x=0.5$, as well as the decrease of the magnitude of the Kondo effect in $\rho(T)$ and $S(T)$ in this concentration range indicate that T_K (or T_f) also decreases with x for $x < 0.7$, in contrast to the constant T_K suggested by Levin *et al.*⁸ Thus, these results indicate a continuous decrease of T_K or T_f from pure EuCu_2Si_2 to EuCu_2Ge_2 , T_K being of the order of 10–30 K at the onset of magnetic order.

C. Valence changes

In order to get more precise information about the valence state of Eu close to the magnetic-nonmagnetic transition, the photoemission measurements on pure EuCu_2Ge_2 and EuCu_2Si_2 and on the compounds with $x=0.6$ and $x=0.7$ were performed both in ultraviolet photoemission spectroscopy (UPS) and x-ray photoemission spectroscopy (XPS) modes. Since the purpose of this work is to study bulk properties of the compounds, in the following we will concentrate on the results of the more bulk-sensitive XPS measurements. The UPS results, which are in agreement with the XPS data, providing additional information on the surface properties of the samples, will be discussed elsewhere.²⁰

The Eu valence in the above compounds was studied by recording the Eu $3d$ and $4f$ core-level PE spectra with the bulk-sensitive Al $K\alpha$ excitation. Due to the large Coulomb-correlation energy, the energy positions of the core-level signals for $4f$ configurations with different electron occupations are shifted by several eV with respect to each other. Therefore, the contributions to the PE from the different $4f$ con-

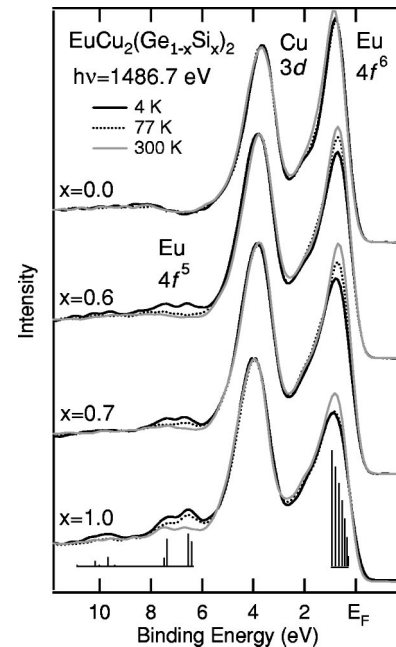


FIG. 8. $4f$ XPS spectra of selected samples. The $x=0.0$ sample is characterized by only the $4f^6$ final-state PE multiplet indicating stable divalent configuration, whereas the other samples reveal additionally the $4f^5$ final-state multiplet providing evidence for valence fluctuation. As a result the relative intensities of the divalent and trivalent components vary for the samples with $x=0.6$, 0.7 , and 1.0 . The $4f^5$ and $4f^6$ multiplets from Ref. 23 are shown by vertical bars at the bottom of the figure.

figurations can easily be discriminated. From the intensity ratio of these contributions the information about the valence can be derived.²¹

The results obtained in the present study from the analysis of the Eu $3d$ and the $4f$ core-level spectra are qualitatively similar to each other. The spectra of the lower-binding energy (BE) $4f$ states reveal, however, much weaker broadening of the $4f$ final-state multiplets (only 10–100 meV) due to the larger lifetime of the core-hole excitation. Therefore, as a rule they allow for more precise assignments of the experimental data as compared to the spectra of the much deeper-lying $3d$ levels. Apart from that the $4f$ spectra can be used for the analysis of the electronic structure close to the Fermi energy (E_F). If the leading $4f$ component of the final-state PE multiplet is observed at the Fermi energy, it shows that this term of the final-state multiplet is energetically degenerate with the ground state and gives, therefore, evidence for homogeneous mixed-valent behavior of the system. The $4f$ energy distribution curves taken at three different temperatures: 300 K (gray curves), 77 K (dotted), and 4 K (black) for the samples doped with different concentrations of Si are shown in Fig. 8. All spectra are normalized to the intensity of the Cu $3d$ valence-band signal (at 3.8 eV BE) that is supposed to be constant within the used range of temperatures and for all four samples differing from each other only by the relative Ge/Si content. The $4f^6$ final-state multiplet corresponding to divalent Eu^{2+} is usually located within the first 2 eV below E_F , while the broad $4f^5$ multiplet of Eu^{3+} is found between 6 and 11 eV binding energies.²²

The $4f$ XPS spectra acquired for EuCu_2Ge_2 at different temperatures (Fig. 8) reveal a prominent peak at about 0.7 eV BE corresponding to a signal from a bulk Eu^{2+} configuration, which is consistent with the pure divalent nature of Eu in EuCu_2Ge_2 . A weak shoulder at the left side of the peak is due to the contribution of divalent surface Eu atoms. The signal around 8 eV BE that does not change with the temperature is related to a plasmon loss structure.²⁴ The intensity of the Eu^{2+} peak is strongly decreased in the spectra of the EuCu_2Si_2 compound. The respective $4f$ spectral weight is transferred into the region of the Eu^{3+} multiplet. This redistribution of the spectral weight is clearly seen particularly in the region of 6–7.5 eV, which is not masked by the contribution of the plasmon-loss structure. Such behavior is in accordance with the valence fluctuating state of this compound. Similar to EuCu_2Si_2 , for the samples with $x=0.6$ and $x=0.7$, both Eu^{2+} and Eu^{3+} contributions are clearly visible indicating a valence fluctuating Eu state. Since the Eu^{2+} component is found to be very close to the Fermi energy, a homogenous mixed-valent origin of the last three compounds can be concluded.

In pure EuCu_2Si_2 the Eu^{2+} signal is strongly suppressed as compared to its value in $\text{EuCu}_2(\text{Ge}_{0.3}\text{Si}_{0.7})_2$. Note also that for the $x=0.7$ sample this signal is slightly weaker than for the $x=0.6$ sample. As expected, the intensities of the Eu^{3+} component follow opposite behavior. Since the intensity variation of the $4f$ final-state multiplets is related with the valence of the rare earth, the observed behavior reflects a strong reduction of the valence between $x=1$ and $x=0.7$ and a weaker decrease between $x=0.7$ and $x=0.6$. This finding is in accordance with the results obtained by our thermodynamic and transport experiments. The latter results are further confirmed by the temperature dependence of the $4f$ spectra. The signal of the Eu^{2+} component does not show significant change with temperature for the stable divalent compound EuCu_2Ge_2 . In contrast to this, the intensity ratio of the Eu^{2+} and the Eu^{3+} components decreases quite significantly with temperature for the valence fluctuating samples with $x=0.6$, 0.7, and 1.0. Note that for pure EuCu_2Si_2 the corresponding changes are more pronounced in the temperature range between 300 K and 77 K than between 77 K and 4 K, whereas for the $x=0.7$ and particularly the $x=0.6$ samples the situation is reversed as expected for a decrease of the characteristic valence fluctuation energy scale.

In order to determine the absolute valence of Eu, we analyzed the intensity ratios of the divalent and trivalent Eu components in the valence-band (Fig. 8) and the Eu $3d$ core-level XPS spectra (not shown). The latter consists of two spin-orbit doublets that correspond to $3d^9 4f^6$ and $3d^9 4f^7$ final states, respectively, and are separated from each other by 6 eV. In spite of this large energy separation data, analysis is complicated by the fact that at a mean kinetic energy of 450 eV, emissions of the divalent outermost atomic layer contribute by about 20–25% to the spectral intensity and a high binding energy component of the $3d^9 4f^7$ multiplet overlaps with the $3d^9 4f^6$ final states.²⁵ To take into account these effects spectra of EuCu_2Ge_2 (our experiment) and

TABLE II. Eu valence ν for different compositions at selected temperatures as determined from the analysis of the Eu $4f$ XPS spectra.

x	ν (300 K)	ν (77 K)	ν (4 K)
1.0	2.10	2.20	2.28
0.7	2.04	2.06	2.15
0.6	2.04	2.05	2.15

EuPd_3 (from Ref. 26) were taken as references for the signals of ideal divalent and trivalent systems. Note, that the relative intensity of the surface component varies slightly as a function of material properties and surface quality and is particularly large in the case of the EuPd_3 spectrum used. As a consequence, the mean valence derived from the $3d$ XPS spectra might be slightly overestimated. In case of the $4f$ spectra in Fig. 8 surface contributions are almost negligible due to the much larger kinetic energy of the photoelectrons. Data analysis, however, is complicated by valence-band contributions and a broad structure of the $4f^5$ final-state multiplet. Within the error of the data evaluation, the values of the mean valence deduced from the $4f$ spectra reproduce the ones obtained from the $3d$ core-level data.

The resulting valencies given in Table II are remarkably smaller than those reported from x-ray absorption (XAS) data^{8,12,32}. The deviations are even larger than the Mössbauer studies^{27,28} where a nearly trivalent state of Eu was reported for EuCu_2Si_2 . Mössbauer experiments are purely bulk sensitive and do not affect directly the electronic states. Thus, the observed deviations may be ascribed to (i) change of crystal structure and stoichiometry in the subsurface region or (ii) final-state effects of the photoemission process. Particularly for the low temperatures applied here lattice relaxations and segregation effects are rather unlikely, and from the similarity of the results obtained from the $3d$ and $4f$ spectra mechanism (i) seems to be not very probable. Mechanism (ii) implies that the final states observed in the photoemission spectra are not characterized by integer $4f$ occupation numbers, but that strong configurational mixing takes place like in Ce and other light rare-earth systems. In this case the simple procedure applied here to determine that the valence leads to rather approximate results and a more sophisticated analysis in the light of the single-impurity Anderson model might be more appropriate. Such an analysis, however, is beyond the scope of the present work.

From the above results we derive the important conclusions that valence fluctuations are not only present for $x > x_c$ in the $x=0.7$ sample showing heavy fermion behavior, but still persist for $x < x_c$ in the $x=0.6$ sample, which is characterized by a well defined long range magnetic order. Thus, a coexistence of well defined long-range magnetic ordering and valence fluctuation is observed. In their theoretical study Bulk and Nolting²⁹ have shown that this is possible in the case of rather weak valence fluctuation. Indeed coexistence of antiferromagnetism and valence fluctuation was observed earlier in Eu metal and in $\text{Eu}(\text{Pd}_{0.8}\text{Au}_{0.2})_2\text{Si}_2$ using high-pressure Mössbauer spectroscopy.^{30,31} In the present study exploiting different kinds of experimental techniques

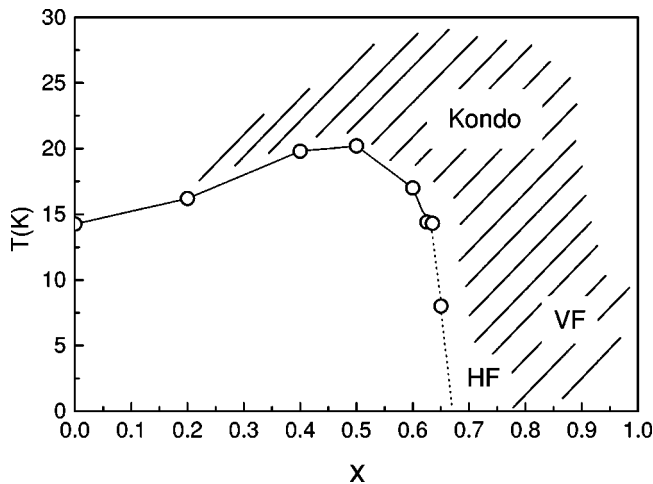


FIG. 9. Magnetic phase diagram of $\text{EuCu}_2(\text{Ge}_{1-x}\text{Si}_x)_2$. Solid line is a guide to eye for T_N s up to $x=0.6375$ which are characterized by well-defined anomalies in specific heat. For $x=0.65$, we found only a broad anomaly centered around 8 K, hence connected by a dotted line. Close to the magnetic-nonmagnetic boundary the system shows Kondo effect and heavy fermion behavior, while for larger x the system exhibits valence fluctuation.

at ambient pressure we were able to show that these valence fluctuations are also consistent with the Kondo-like behavior of the resistivity and the thermopower.

IV. SUMMARY

Our results are summarized in the magnetic phase diagram shown in Fig. 9. Our specific heat, susceptibility, and resistivity results confirm an antiferromagnetic state in pure EuCu_2Ge_2 with a SDW-like anomaly in $\rho(T)$ at $T_N=14$ K. The long-range antiferromagnetic order is stable until a critical point at $x=0.65$. T_N first increases with Si content, up to $T_N=20$ K around $x=0.5$, but shows then a significant decrease with further increasing x , down to $T_N=14$ K at $x=0.6375$. We cannot tell unambiguously whether the AF state disappears at a quantum critical point ($T_N \rightarrow 0$ K) or at

a classical critical point at a finite temperature [$T_N(x \rightarrow x_c) \rightarrow 13$ K]. For x slightly larger than x_c , we observe the formation of a heavy Fermi liquid at low temperatures, as evidenced by a large linear coefficient in the specific heat ($\gamma = 191$ mJ/K² mol for $x=0.7$), T^2 dependence of resistivity with a large coefficient A , and a strongly enhanced constant susceptibility χ_0 . Both the Wilson's ratio χ_0/γ and the Kadowaki-Woods ratio A/γ^2 show the value expected for a heavy fermion system. Kondo-like behavior appears in the temperature dependence of the resistivity and of the thermopower for $x > 0.4$, and becomes very pronounced around x_c . For further increasing Si content, the systems evolve towards valence fluctuating properties. The thermopower data suggest a continuous decrease of the Kondo scale (or the characteristic fluctuation energy scale) from pure EuCu_2Si_2 to EuCu_2Ge_2 . The temperature and concentration dependence of XPS and UPS results indicate that valence fluctuation persists from $x=1$ down to at least $x=0.6$, well into the antiferromagnetic regime.

We presented here experimental evidence for heavy fermion behavior and coexistence of valence fluctuation and magnetic order at ambient pressure in Eu compounds. The heavy fermion behavior in this case is unique as the eight fold degeneracy of the divalent Eu ($4f^7$; $J=S=7/2$) is preserved down to lowest temperature in contrast to the Ce-, Yb-, or U-based heavy fermions where the effective degeneracy is lowered due to crystal field splitting. As the number of f electrons is rather large, it might be possible to find experimental evidence for underscreened Kondo effect. Such studies shall be one of the focus of further research.

ACKNOWLEDGMENTS

The work was supported by the Deutsche Forschungsgemeinschaft, Grants Nos. SFB 463, TP B14 and B16. We thank V. H. Tran and S. Paschen for their support in thermopower measurements and discussion of the results. We also thank R. Ramlau for electron probe microanalysis. Fruitful discussions with V. Zlatić, F. Steglich, C. Laubschat, M. B. Maple, B. Coqblin, and J. Mydosh are gratefully acknowledged.

¹F. Steglich, *J. Magn. Magn. Mater.* **226-230**, 1 (2001).

²N.D. Mathur, F.M. Grosche, S.R. Julian, I.R. Walker, D.M. Freye, R.K.W. Haselwimmer, and G.G. Lonzarich, *Nature (London)* **394**, 39 (1998).

³R. Movshovich, T. Graf, D. Mandrus, J.D. Thompson, J.L. Smith, and Z. Fisk, *Phys. Rev. B* **53**, 8241 (1996).

⁴F.M. Grosche, I.R. Walker, S.R. Julian, N.D. Mathur, D.M. Freye, M.J. Steiner, and G.G. Lonzarich, *J. Phys.: Condens. Matter* **13**, 2845 (2001).

⁵G.R. Stewart, *Rev. Mod. Phys.* **73**, 797 (2001).

⁶H. Wada, A. Nakamura, A. Mitsuda, M. Shiga, T. Tanaka, H. Mitamura, and T. Goto, *J. Phys.: Condens. Matter* **9**, 7913 (1997).

⁷C.U. Segre, M. Croft, J.A. Hodges, V. Murgai, L.C. Gupta, and R.D. Parks, *Phys. Rev. Lett.* **49**, 1947 (1982).

⁸E.M. Levin, B.S. Kuzhel, O.I. Bodak, B.D. Belan, and I.N. Stets, *Phys. Status Solidi B* **161**, 783 (1990).

⁹I. Felner and I. Nowik, *J. Phys. Chem. Solids* **39**, 763 (1978).

¹⁰B.C. Sales and R. Viswanathan, *J. Low Temp. Phys.* **23**, 449 (1976).

¹¹E.M. Levin, T. Palewski, and B.S. Kuzhel, *Physica B* **294-295**, 267 (2001).

¹²S. Fukuda, Y. Nakanuma, A. Mitsuda, Y. Ishikawa, and J. Sakurai, *Acta Phys. Pol. B* **34**, 1177 (2003).

¹³A.R. Mackintosh, *Phys. Rev. Lett.* **9**, 90 (1962).

¹⁴J.A. Blanco, D. Gignoux, and D. Schmitt, *Phys. Rev. B* **43**, 13 145 (1991).

¹⁵K. Kadowaki and S.B. Woods, *Solid State Commun.* **58**, 507 (1986).

¹⁶N. Tsujii, K. Yoshimura, and K. Kosuge, *J. Phys.: Condens. Mat-*

- ter **15**, 1993 (2003).
- ¹⁷H. Kontani, cond-mat/0308484 (unpublished).
- ¹⁸V.T. Rajan, Phys. Rev. Lett. **51**, 308 (1983)
- ¹⁹V. Zlatić (private communication).
- ²⁰F. Schiller *et al.* (unpublished).
- ²¹C. Laubschat, B. Perscheid, and W.-D. Schneider, Phys. Rev. B **28**, 4342 (1983).
- ²²W.D. Schneider, C. Laubschat, G. Kalkowski, J. Haase, and A. Puschmann, Phys. Rev. B **28**, 2017 (1983), and references therein.
- ²³F. Gerken, Ph.D. thesis, University of Hamburg, 1982.
- ²⁴R. Wahl, W. Schneider, S.L. Molodtsov, S. Danzenbächer, C. Laubschat, M. Richter, and E. Weschke, Phys. Rev. Lett. **82**, 670 (1999).
- ²⁵W.J. Lademan, A.K. See, L.E. Klebanoff, and G. van der Lann, Phys. Rev. B **54**, 17 191 (1996).
- ²⁶W.-D. Schneider, C. Laubschat, I. Nowik, and G. Kaindl, Phys. Rev. B **24**, 5422 (1981).
- ²⁷E.R. Bauminger, D. Froindlich, I. Nowik, and S. Ofer, Phys. Rev. Lett. **30**, 1053 (1973).
- ²⁸A. Scherzberg, C. Sauer, U. Köbler, W. Zinn, and J. Röhler, Solid State Commun. **49**, 1027 (1984).
- ²⁹G. Bulk and W. Nolting, Z. Phys. B: Condens. Matter **70**, 473 (1988).
- ³⁰J.N. Farrell and R.D. Taylor, Phys. Rev. Lett. **58**, 2478 (1987).
- ³¹M.M. Abd-Elmeguid, Ch. Sauer, and W. Zinn, Phys. Rev. Lett. **55**, 2467 (1985).
- ³²In this context, we notice that the valence obtained from XAS measurement by Fukuda *et al.* (Ref. 12) are significantly higher than those obtained by Levin *et al.* (Ref. 8).